HHS Public Access

Author manuscript

Mol Imaging Biol. Author manuscript; available in PMC 2019 May 27.

Published in final edited form as:

Mol Imaging Biol. 2018 April ; 20(2): 221–229. doi:10.1007/s11307-017-1109-3.

Sentinel Lymph Node Characterization with a Dual-Targeted Molecular Ultrasound Contrast Agent

Kibo Nam[1], **Maria Stanczak**[1], **Flemming Forsberg**[1], **Ji-Bin Liu**[1], **John R. Eisenbrey**[1], **Charalambos C. Solomides**[2], and **Andrej Lyshchik**[1]

[1]Department of Radiology, Thomas Jefferson University, 132 South 10th Street, Philadelphia, PA, 19107, USA

[2]Department of Pathology, Thomas Jefferson University, Philadelphia, PA, 19107, USA

Abstract

Purpose: The purpose of this study was to assess the performance of molecular ultrasound with dual-targeted microbubbles to detect metastatic disease in the sentinel lymph nodes (SLNs) in swine model of naturally occurring melanoma. The SLN is the first lymph node in the lymphatic chain draining primary tumor, and early detection of metastatic SLN involvement is critical in the appropriate management of melanoma.

Procedure: Nine Sinclair swine (weight 3–7 kg; Sinclair BioResources, Columbia, MO, USA) with naturally occurring melanoma were examined. Siemens S3000 scanner with a 9L4 probe was used for imaging (Siemens Healthineers, Mountain View, CA). Dual-targeted contrast agent was created using Targestar SA microbubbles (Targeson, San Diego, CA, USA) labeled with $\alpha_v\beta_3$-integrin and P-selectin antibodies. Targestar SA microbubbles labeled with IgG-labeled were used as control. First, peritumoral injection of Sonazoid contrast agent (GE Healthcare, Oslo, Norway) was performed to detect SLNs. After that, dual-targeted and IGG control Targestar SA microbubbles were injected intravenously with a 30-min interval between injections. Labeled Targestar SA microbubbles were allowed to circulate for 4 min to enable binding. After that, two sets of image clips were acquired several seconds before and after a high-power destruction sequence. The mean intensity difference pre- to post-bubble destruction within the region of interest placed over SLN was calculated as a relative measure of targeted microbubble contrast agent retention. This process was repeated for non-SLNs as controls. All lymph nodes evaluated on imaging were surgically removed and histologically examined for presence of metastatic involvement.

Correspondence to: Andrej Lyshchik; andrej.lyshchik@jefferson.edu.

Compliance with Ethical Standards. This study was approved by the Thomas Jefferson University Animal Care and Use Committee and was performed in accordance with the guidelines of the National Institutes of Health and supervised by our Laboratory Animal Services Department guidelines.

Conflict of Interest

Dr. Forsberg is on the Speaker's Bureau of GE Healthcare, and Dr. Eisenbrey receives funding, equipment, and drug support from GE Healthcare. The other authors declare that they have no relevant conflict of interest.

Ethical Approval

All applicable institutional and/or national guidelines for the care and use of animals were followed.

Results: A total of 43 lymph nodes (25 SLNs and 18 non-SLNs) were included in the analysis with 18 SLNs demonstrating metastatic involvement greater than 5 % on histology. All non-SLNs were benign. The mean intensity (± SD) of the dual-targeted microbubbles for metastatic SLNs was significantly higher than that of benign LNs (18.05 ± 19.11 *vs.* 3.30 ± 6.65 AU; $p = 0.0008$), while IgG-labeled control microbubbles demonstrated no difference in retained contrast intensity between metastatic and benign lymph nodes (0.39 ± 1.14 *vs.* 0.03 ± 0.24 AU; $p = 0.14$).

Conclusions: The results indicate that dual-targeted microbubbles labeled with P-selectin and $\alpha_v\beta_3$-integrin antibodies may aid in detecting metastatic involvement in SLNs of melanoma.

Keywords

Sentinel lymph nodes; Characterization; Melanoma; Metastasis; Ultrasound; Contrast imaging; Targeted microbubbles; Angiogenesis; Inflammation

Introduction

Although melanoma is not as common as other types of skin cancer, it is usually more aggressive and tends to grow and spread [1]. The lifetime risk of melanoma is about 1 in 40 for Caucasians, 1 in 1000 for African-Americans, and 1 in 200 for Hispanics [1]. For early-stage melanoma, the estimated 5-year survival rate in the USA range from 81 to 97 % [1]. Unfortunately, the rate of survival rate drops to 40–78 % in patients with melanoma spread to the regional lymph nodes and to 15–20 % in patients with distant metastasis [1]. Thus, early detection and proper characterization of metastatic involvement of lymph nodes is critical for appropriate clinical management [2].

According to the current clinical care standards, metastatic lymph node involvement is identified by a sentinel lymph node (SLN; the first node in the lymphatic chain draining a primary tumor) biopsy and completion lymphadenectomy [3]. A SLN biopsy is an invasive surgical procedure. It is composed of two parts: lymphatic mapping and surgical excision. To map SNL, physicians perform preoperative lymphoscintigraphy to identify areas of increased radiotracer accumulation outside of the tumor. Then, surgeons inject a blue dye near the site of the tumor and detect SLNs with a Geiger counter and blue dyes. After that, surgical resection of the SLNs is performed and resected specimens are used to assess the presence of metastatic disease in the lymph nodes [4]. A SLN biopsy has some limitations. Since lymphoscintigraphy utilizes a radioisotope, some clinics may not have the necessary capabilities [5]. Also, allergic/anaphylactic reaction to use of blue dyes has been reported [6]. Moreover, an SLN excision may not be recommended for patients with surgical or anesthesia risks [7].

Contrast-enhanced ultrasound imaging (CEUS) following subdermal or peritumoral injection of microbubble ultrasound contrast agent has been developed to detect lymphatic channels (LCs) and SLNs *in vivo* [8-11]. Our group previously showed that CEUS over-performed lymphoscintigraphy in detecting SLNs, which were identified by blue dye-guided surgery in 63 swine with 104 melanomas [10]. The accuracy of SLN detection was 81.8 % for CEUS and 63.2 % for lymphoscintigraphy [10]. Detected SLNs were characterized by assessing 2D and 3D CEUS images with a accumulation of contrast agent quantitatively and

qualitatively. However, the diagnostic accuracy of characterizing metastatic involvement of SLNs was limited (60–80 %) [10].

To detect metastatic SLN involvement more accurately, targeted ultrasound contrast agents can be used [12-14]. Targeted contrast agents are created by adding ligands onto the surface of the microbubbles to detect specific molecular markers. Avidin or streptavidin is frequently used for non-covalent attachment of biotinylated ligands onto the shell of microbubbles, due to its wide availability and flexibility in pre-clinical research [15]. Increased angiogenesis and inflammation in the tumor and lymph nodes have been known to be associated with melanoma metastasis [16-19]. In the processes of tumor angiogenesis and inflammation, various molecular markers are over-expressed on tumor vascular endothelial cells [15, 20]. Targeted contrast agents were successfully utilized to detect these molecular markers of tumor angiogenesis such as vascular endothelial growth factor receptor type-2 (VEGFR-2), $\alpha_v\beta_3$-integrin, or endoglin [12, 13, 21, 22]. Other studies showed that inflammatory markers such as E- and P-selectin, anti-intercellular adhesion molecule 1 (ICAM-1), and anti-vascular cell adhesion molecule 1 (VCAM-1) could be targeted with microbubbles to quantify inflammation [15, 23-25]. The purpose of this study was to assess the performance of molecular ultrasound with dual-targeted microbubbles to detect metastatic disease in the sentinel lymph nodes of swine with naturally occurring melanoma.

Materials and Methods

This study was approved by the Thomas Jefferson University Animal Care and Use Committee and was performed in accordance with the guidelines of the National Institutes of Health and supervised by our Laboratory Animal Services Department guidelines.

Animal Model

Nine Sinclair swine (weight 3–7 kg) with naturally occurring melanoma tumors were purchased from Sinclair BioResources, (Columbia, MO, USA). This swine model produces tumors similar to human melanomas in their clinical course and histopathologic characteristics with a 70 % rate of SLN metastasis [10]. The night before the experiment, the swine were pre-treated orally with Zantac, 1 mg/kg (Glenmark Generics Inc., Mahwah, NJ, USA) and Benadryl, 2 mg/kg (PRN Pharmacal, Pensacola, FL, USA) to prevent possible allergic reactions. Pre-operatively, the swine were pre-medicated using an intramuscular administration of Atropine, 0.04 mg/kg (Med-Pharmex Inc., Pomona, CA, USA), along with Telazol, 3 mg/kg (Tiletamine/ Zolazepam; Pfizer, New York, NY, USA), Zantac, 1 mg/kg (Zydus Pharmaceuticals, Pennington, NJ, USA), and Benadryl 2 mg/kg (Mylan, Rockford, IL, USA). Also, the swine were pre-treated using an intravenous administration of a non-steroidal anti-inflammatory medication Toradol, 4–5 mg/kg (Genentech, Inc., San Francisco, CA, USA) 20 min prior to the intravenous (IV) injection of the targeted contrast agents. General anesthesia was administered by 2 to 4 % of isoflurane delivered through an endotracheal tube and titrated to effect. Swine body temperature was maintained within normal range by a warming blanket.

Contrast Agents

Table 1 summarizes the type and use of ultrasound contrast agents in this study. Based on previous studies, two-step imaging approach was used [8-10]. First, SNL *identification* was performed using lymphosonography after peritumoral injection of Sonazoid (GE Healthcare, Oslo, Norway). Sonazoid is a lipid stabilized suspension of perfluorobutane microbubbles with a median diameter of 2.4 to 3.5 μm [26]. Then, SLN *characterization* was performed using CEUS after IV injection of targeted microbubbles. Since it was previously demonstrated that expression of angiogenesis markers can vary in different tumor types and at different stages of tumor development, dual-targeted microbubbles were selected to increase the chance of selective contrast agent binding [27]. To select the most appropriate targeting ligand strategy, a total of 12 swine metastatic lymph nodes from a previous study [10] were tested immunohistochemically to estimate relative expression of common endothelial markers (*i.e.*,VEGFR-2, P-selectin, and $\alpha_v\beta_3$-integrin) as a preliminary study.

In creating dual-targeted microbubbles, the anti-$\alpha_v\beta_3$-integrin (Millipore, Billerica MA, USA) and anti-P-selectin (LifeSpan Biosciences, Seattle, WA, USA) antibodies were first biotinylated using a sulfo-NHS-biotin linkage kit (Thermo Scientific, Rockford, IL, USA). The dual-targeted microbubbles were then produced by incubating the streptavidin coated Targestar SA microbubbles (Targeson, San Diego, CA, USA, a median diameter of 1.6 to 2.0 μm) with 50 μg/ml of each biotinylated antibody. Non-targeted control microbubbles were produced by incubating the streptavidin coated Targestar SA microbubbles with 100 μg/ml of biotinylated immunoglobulin G (IgG). It should be noted that although targeted contrast agents produced using avidin-biotin antibody bonding are not directly translatable to humans, it is a cost-effective model and can be easily modified to a conjugation before translation to clinical studies [28].

Ultrasound Imaging

The overview of ultrasound imaging protocol is presented in Fig. 1a. B-mode and CEUS imaging were performed using a Siemens S3000 HELX scanner with a 9L4 linear array probe (Siemens Healthineers, Mountain View, CA, USA) using center frequencies of 6–8 MHz. Baseline B-mode scanning around a melanoma tumor and along the common lymphatic chains was first performed to identify possible regional lymph node involvement. Sonazoid was administered sub-dermally in four separate injections of 0.25 ml each for a total dose of 1.0 ml around each melanoma tumor at 3, 6, 9, and 12 o'clock positions. Immediately after peritumoral Sonazoid injection, tissues around the tumor were gently massaged for up to 5 min to facilitate lymphatic uptake of Sonazoid. SLN identification was then performed using CEUS scanning along the enhancing lymphatic channels originating in the primary tumor. CEUS was performed using Cadence Pulse Sequencing at low acoustic power (MI < 0.1) to minimize Sonazoid microbubble destruction [29]. The locations and sizes of identified SLNs were recorded. Then, Color Doppler imaging through SLN area with high MI was utilized to destroy the residual Sonazoid contrast agent. Insonification was continued until no Sonazoid was left within the LCs and SLNs [10]. After complete clearance of Sonazoid was achieved, dual-targeted and control microbubbles were injected IV. Injections were performed in random order with a 30-min interval between injections. After injection, each microbubbles were allowed to circulate for 4 min to enable binding.

Then, two sets of image clips (each 4 s long) were collected for identified SLNs immediately before and after high MI destruction sequence (MI > 0.8, center frequency 4 MHz). The clearance of microbubbles from the circulation between IV injections was confirmed by a RDMS certified sonographer (MS with 20+ years of experience). As control, some non-SLNs identified on baseline imaging of lymphatic chains distant to the primary tumor were also imaged with dual-targeted and control microbubbles. All imaging parameters were kept constant, while imaging with targeted and control microbubbles was performed.

Molecular Ultrasound Data Analysis

The collected SLN characterizetion image clips were digitally stored and transferred to a PC for offline analysis. Pre-destruction images (50–100 frames) were selected from the images recorded after the microbubbles' possible binding (4 min after IV contrast injection) and before the ultrasound contrast agent destruction pulse. The post-destruction images (50–100 frames) were selected from images collected after the free circulating ultrasound contrast agent refilling and before any possible re-binding *(i.e.*, within 10 s after the destruction pulse). Image analysis was performed using Matlab R2015b (Mathworks, Natick, MA, USA). The mean ultrasound contrast agent signal intensity within the region of interest placed over each lymph node was calculated in each image. The results were averaged over the predestruction and post-destruction images. Then, the mean intensity difference between pre- and post-destruction images was calculated and used as a relative measure of targeted ultrasound contrast agent retention in the lymph nodes [30].

All examined SLNs and non-SLNs were surgically removed and histologically examined for the presence of metastatic involvement. Histopathologic analysis was performed on the H&E stained slides by a pathologist (C. C. S) with 30 years of experience. The relative bubble retention measures from dual-targeted and control microbubbles for each lymph node were compared to the presence of metastatic involvement on histology. A Student's *t* test was used to compare the relative retention of dual-targeted and control microbubbles in the metastatic and benign lymph nodes. Also, a nested ANOVA was performed to compare the microbubble retention of lymph nodes under the subgroups of pigs. MatLab was used for all statistical analyses with a 5 % significance level indicating statistical significance.

Results

The antibodies used in this study were selected based on their documented reactivity in swine. Immunohistological analysis showed that the expressions of $\alpha_v\beta_3$-integrin and P-selectin were approximately 10 % higher than that of VEGFR-2 (data not shown). Hence $\alpha_v\beta_3$-integrin and P-selectin were selected to create a dual-targeted contrast agent for this study.

A total of 43 lymph nodes (25 SLNs and 18 non-SLNs) were examined. There were one swine with two tumors (located near the neck and the tail), one swine with three tumors (located near the neck, face, and the foot) while the other animals had one tumor (Fig. 1b). After Sonazoid administration, SLNs were identified by CEUS in all animals. The LCs and SLNs in all animals demonstrated substantial enhancement after peritumoral Sonazoid administration and were easily visualized (Fig. 2).

The scanning position between imaging with targeted and control microbubbles were maintained as much as possible. The depths of lymph nodes in the targeted and control microbubble images ranged from 0.2 to 2.3 cm (median 0.7 cm) and from 0.2 to 2.5 cm (median 0.8 cm), respectively. The sizes of lymph nodes in the CEUS images with targeted and control microbubbles were 0.14–5.70 cm^2 (median 0.59 cm^2) and 0.16–4.63 cm^2 (median 0.57 cm^2), respectively.

All examined lymph nodes were surgically removed and assessed by histopathology for metastatic involvement. Among the 25 SLNs, 18 SLNs demonstrated metastatic melanoma involvement greater than 5 % and were considered malignant. All 18 non-SLNs were benign. The mean ultrasound contrast agent signal intensity (±SD) of the dual-targeted microbubbles in metastatic nodes was significantly higher than that of benign nodes (18.05 ± 19.11 *vs.* 3.30 ± 6.65 AU; $p = 0.0008$), while IgG control microbubbles did not show significant difference in signal intensities of retained microbubbles between metastatic and benign nodes (0.39 ± 1.14 *vs.* 0.03 ± 0.24 AU; $p = 0.14$). The mean intensities from dual-targeted and control microbubbles for metastatic and benign nodes are presented in Fig. 3. Additionally, metastatic SLNs showed large differences between targeted and control microbubbles as demonstrated in Fig. 4 ($p = 0.0004$). Benign nodes also showed a difference in the mean intensity between dual-targeted and control microbubbles ($p = 0.0012$). Overall, mean intensities of both dual-targeted and control microbubbles were much lower in benign nodes than in metastatic nodes (*cf.*, Fig. 5). An example of a benign node imaged with the two types of microbubbles is presented in Fig. 5. A nested ANOVA showed that the mean intensities of IgG microbubbles were not different ($p = 0.85$) among pigs while those of dual-targeted microbubbles were significantly different ($p = 0.0032$). It also demonstrated that dual-targeted microbubbles differentiated metastatic LN from benign($p = 0.001$) while IgG microbubbles did not differentiate them ($p = 0.65$).

Discussion

Detecting metastasis in SLNs is critical for the appropriate clinical management of patients with melanoma [2, 3]. Specifically, SLN involvement has been shown to be a strong prognostic indicator with less than a 5 % patients diagnosed with a negative SLN presenting with a positive non-SLN [31]. Currently, SLN biopsy is a commonly used tool for evaluating SLNs [32]. SLN biopsy is invasive and carries a substantial morbidity risk. The adverse effect of lymph node resection includes lymphedema, seroma, numbness, tingling, or pain at the site of the surgery [32]. There is, however, a controversy about when to perform biopsies in patients with melanomas less than 1 mm due to less favorable risk-to-benefit ratio of SLN biopsy in this group [33]. Thus, non-invasive and radiation-free method of SLN detection and characterization would be beneficial for all melanoma patients.

Recently multispectral optoacoustic tomography (MSOT) was introduced to assess SLN metastatic status *ex vivo* (148 SLNs from 65 patients) and *in vivo* (41 SLNs from 20 patients) in patients with melanoma [34]. The study showed the feasibility of using photoacoustic techniques to detect and characterize melanoma SLNs, but specificity was limited to 48 and 62 % for *ex vivo* and *in vivo* applications, respectively [34]. The main limitation is that MSOT detects SLN metastasis based on melanin level [34]. It did not detect

metastatic deposits of amelanotic melanomas from four patients [34]. Our group has previously developed and validated method of SLNs identification with peritumoral injection of Sonazoid contrast agent [8-10]. The same strategy was used to detect SLNs in this study, and SLNs were identified by following the enhanced LCs. Sonazoid is a reticuloendothelial-specific ultrasound contrast agent and performs extremely well for this novel lymphatic system application [10].

However, our previous results demonstrated limited accuracy in characterization of SLNs with Sonazoid [10]. The aim of this study was to improve accuracy of SLN characterization using CEUS after intravenous injection of dual-targeted microbubbles allowing detection of angiogenesis and inflammation within the SLNs. In several studies, targeted contrast agents have been successfully applied for the detection of neovasculature [35-37] and inflammation [38, 39] as well as other purposes [40, 41]. Nonetheless, the application of targeted microbubbles to lymph nodes has been rather limited [42, 43]. Dewitte el al. [42] showed that homemade unloaded and mRNA-loaded microbubbles reached the LCs and nodes upon subcutaneous injection in dogs. Hauff et al. evaluated the feasibility of using intravenously administered microbubbles labeled with L-selectin to detect peripheral lymph nodes in healthy mice and dogs [43]. The lymph nodes of mice (cervical, inguinal, axial, popliteal, mesenteric) and dogs (popliteal) were assessed with harmonic color Doppler *ex vivo* and *in vivo* after injection of the microbubbles. The targeted microbubbles were found in all monitored LNs of mice and dogs [43]. To the best of our knowledge, this study is the first that have attempted to perform LN characterization using molecular imaging with dual-targeted ultrasound contrast agent.

In previous studies [27, 44], dual-targeted microbubbles showed higher adherence than single-targeted microbubbles for mouse SVR breast cancer model *in vivo* and *in vitro,* respectively. The latter *in vitro* study [44] also reported that triple-targeted microbubbles demonstrated the highest adherence compared to single- and dual-targeted microbubbles. In that study [44], the triple-targeted targeted microbubbles were labeled with antibodies of $\alpha_v\beta_3$-integrin, P-selectin, and VEGFR-2. However, in our pathology analysis, P-selectin and $\alpha_v\beta_3$-integrin showed increased expression in excised metastatic swine nodes relative to VEGFR-2. Moreover, another study with human melanoma cases [45] found that less than 10 % of melanoma cells expressed detectable levels of VEGFR-2 with immunohistochemistry analysis. Because binding sites per microbubble are limited, dual targeted microbubbles were utilized in this study to maximize microbubble attachment.

During the two-stage approach, *i.e.*, detection of SLNs and characterization of SLNs, adopted in this study, the types of contrast agents and their injection sites differed. Sonazoid used for detection of SLNs was injected subcutaneously around the tumor, while dual-targeted microbubbles (or control bubbles) used for characterization of the identified SLNs were injected intravenously. Other studies [8-10, 46-48] used various ultrasound contrast agents and injected them subcutaneously as tracers to detect SLNs. Subcutaneously injected contrast agents were expected to drain through the lymphatic pathway and all these studies detected SLNs. In addition, some studies [8-10, 47, 48] reported that SLNs and LCs were visualized with ultrasound contrast agents and our study confirmed these findings. However, in previous studies, the ultrasound contrast agents used to detect metastatic involvement in

the lymph nodes were injected IV, since metastatic lymph nodes may exhibit peripheral and mixed vascularity due to tumor angiogenesis [49-51]. Thus, ultrasound contrast agents injected IV were intended to enhance the micro- and neo-vessels in the lymph nodes. The dual-targeted microbubbles used in this study were designed to target tumor angiogenesis actively following IV injection.

We have demonstrated that retention of dual-targeted bubbles within metastatic lymph nodes was significantly higher than in benign lymph nodes, while the retention of IgG control microbubbles did not show any significant difference. These findings are in agreement with previous studies that found increased levels of angiogenesis in metastatic SLN [16, 52, 53]. Though it was not statistically significant, IgG control microbubbles showed a slightly higher bubble retention value for metastatic nodes than for benign nodes. It could be because there were more blood vessels in the metastatic nodes. It was also observed that the dual-targeted bubbles (3.30 ± 6.65 AU) were retained more in benign nodes than control microbubble (0.03 ± 0.24 AU). This could be caused by inflammation in some benign nodes [54, 55]. In the future, the dual-targeted bubble retention measure will also be compared to results from immunohistochemical or immunohistofluorescent analyses of angiogenesis. It was also noted that the mean intensities from dual-targeted microbubbles were different among pigs while those from control microbubbles were not. This might be because the metastatic stages of lymph nodes were varied among pigs. The binding sensitivity to the microvasculature within lymph nodes could be higher for dual-targeted microbubbles than for control microbubbles based on their overall retention differences (*i.e.* high *vs.* low).

One of the limitations of this pilot study was the relatively small number of SLNs studied. Nonetheless, the results do provide an indication for a future larger study. Another limitation is that the detection of SLNs was not verified with a reference method. The standard method to detect SLNs is a combination of blue-dye-guided surgery and lymphoscintigraphy [1, 10]. Goldberg et al. used blue-dye-guided surgery as a reference method and showed that lymphosonography with Sonazoid had a higher accuracy (81.8 %) in detecting SLNs (380 identified SLNs) than lymphoscintigraphy (63.2 %) [10]. The blue-dye-guided surgery missed 29 SLNs, which were detected with both of lymphosonography and lymphoscintigraphy and its accuracy was thus 92.4 %. Because this study focused on characterization of detected lymph nodes, the verification of detected SLNs was omitted given the previous study [10]. Finally, the mean intensities from lymph nodes did not accounted for any differences in depth.

Conclusions

Lymphosonography with Sonazoid showed the ability to identify SLNs of melanoma by following the enhanced LCs in all cases. In addition, molecular imaging with intravenous administration of dual-targeted microbubbles labeled with P-selectin and $\alpha_v\beta_3$-integrin antibodies demonstrated potential to characterize metastatic involvement in SLNs in swine model with naturally occurring melanoma.

Acknowledgements.

Joseph Altemus, a lab animal veterinary technician in Thomas Jefferson University, is specifically acknowledged for help with animal care. This study was supported by NIH R21 CA185121 and GE Healthcare provided Sonazoid, while Siemens provided the S3000 HELX scanner. However, the authors had sole control of the data and information provided for publication.

References

1. American Cancer Society (2017) Melanoma skin cancer. http://www.cancer.org/cancer/skincancer-melanoma. Accessed 6 April 2017
2. Morton DL, Thompson JF, Cochran AJ et al. (2006) Sentinel-node biopsy or nodal observation in melanoma. N Engl J Med 355:1307–1317 [PubMed: 17005948]
3. Balch CM, Gershenwald JE, Soong SJ et al. (2009) Final version of 2009 AJCC melanoma staging and classification. J Clin Oncol 27:6199–6206 [PubMed: 19917835]
4. Han D, Thomas DC, Zager JS et al. (2016) Clinical utilities and biological characteristics of melanoma sentinel lymph nodes. World J Clin Oncol 7:174–188 [PubMed: 27081640]
5. Li C, Meng S, Yang X et al. (2015) Sentinel lymph node detection using magnetic resonance lymphography with conventional gadolinium contrast agent in breast cancer: a preliminary clinical study. BMC Cancer 15:213 [PubMed: 25886638]
6. Montgomery LL, Thorne AC, Van Zee KJ et al. (2002) Isosulfan blue dye reactions during sentinel lymph node mapping for breast cancer. Anesth Analg 95:385–388 [PubMed: 12145056]
7. Phan GQ, Messina JL, Sondak VK, Zager JS (2009) Sentinel lymph node biopsy for melanoma: indications and rationale. Cancer Control 16:234–239 [PubMed: 19556963]
8. Goldberg BB, Merton DA, Liu JB et al. (2005) Contrast-enhanced sonographic imaging of lymphatic channels and sentinel lymph nodes. J Ultrasound Med 24:953–965 [PubMed: 15972710]
9. Goldberg BB, Merton DA, Liu JB et al. (2004) Sentinel lymph nodes in a swine model with melanoma: contrast-enhanced lymphatic US. Radiology 230:727–734 [PubMed: 14990839]
10. Goldberg BB, Merton DA, Liu JB et al. (2011) Contrast-enhanced ultrasound imaging of sentinel lymph nodes after peritumoral administration of Sonazoid in a melanoma tumor animal model. J Ultrasound Med 30:441–453 [PubMed: 21460143]
11. Sever A, Broillet A, Schneider M et al. (2010) Dynamic visualization of lymphatic channels and sentinel lymph nodes using intradermal microbubbles and contrast-enhanced ultrasound in a swine model and patient with breast cancer. J Ultrasound Med 29:1699–1704 [PubMed: 21098840]
12. Lyshchik A, Fleischer AC, Huamani J et al. (2007) Molecular imaging of vascular endothelial growth factor receptor 2 expression using targeted contrast enhanced high-frequency ultrasonography. J Ultrasound Med 26:1575–1586 [PubMed: 17957052]
13. Lee DK, Lyshchik A, Huamani J et al. (2008) Relationship between retention of a vascular endothelial growth factor receptor 2(VEGFR2)-targeted ultrasonographic contrast agent and the level of VEGFR2 expression in an in vivo breast cancer model. J Ultrasound Med 27:855–866 [PubMed: 18499845]
14. Kiessling F, Bzyl J, Fokong S et al. (2012) Targeted ultrasound imaging of cancer: an emerging technology on its way to clinics. Curr Pharm Des 18:2184–2199 [PubMed: 22352772]
15. Deshpande N, Needles A, Willmann JK (2010) Molecular ultrasound imaging: current status and future directions. Clin Radiol 65:567–581 [PubMed: 20541656]
16. Pastushenko I, Van den Eynden GG, Vicente-Arregui S et al. (2016) Increased angiogenesis and lymphangiogenesis in metastatic sentinel lymph nodes is associated with nonsentinel lymph node involvement and distant metastasis in patients with melanoma. Am J Dermatopathol 38:338–346 [PubMed: 26909582]
17. Streit M, Detmar M (2003) Angiogenesis, lymphangiogenesis, and melanoma metastasis. Oncogene 22:3172–3179 [PubMed: 12789293]
18. Melnikova VO, Bar-Eli M (2009) Inflammation and melanoma metastasis. Pigment Cell Melanoma Res 22:257–267 [PubMed: 19368690]

19. Wu X, Takekoshi T, Sullivan A, Hwang ST (2011) Inflammation and tumor microenvironment in lymph node metastasis. Cancers 3:927–944 [PubMed: 24212647]
20. Hanahan D, Weinberg RA (2000) The hallmarks of cancer. Cell 100:57–70 [PubMed: 10647931]
21. Daeichin V, Kooiman K, Skachkov I et al. (2016) Quantification of endothelial $\alpha_v\beta_3$ expression with high-frequency ultrasound and targeted microbubbles: in vitro and in vivo studies. Ultrasound Med Biol 42:2283–2293 [PubMed: 27302657]
22. Korpanty G, Carbon JG, Grayburn PA et al. (2007) Monitoring response to anticancer therapy by targeting microbubbles to tumor vasculature. Clin Cancer Res 13:323–330 [PubMed: 17200371]
23. Lindner JR, Song J, Christiansen J et al. (2001) Ultrasound assessment of inflammation and renal tissue injury with microbubbles targeted to P-selectin. Circulation 104:2107–2112 [PubMed: 11673354]
24. Kaufmann BA, Lewis C, Xie A et al. (2007) Detection of recent myocardial ischaemia by molecular imaging of P-selectin with targeted contrast echocardiography. Eur Heart J 28:2011–2017 [PubMed: 17526905]
25. Kaufmann BA, Sanders JM, Davis C et al. (2007) Molecular imaging of inflammation in atherosclerosis with targeted ultrasound detection of vascular cell adhesion molecule-1. Circulation 116:276–284 [PubMed: 17592078]
26. Sontum PC (2008) Physiochemical characteristics of Sonazoid, a new contrast agent for ultrasound imaging. Ultrasound Med Biol 34:824–833 [PubMed: 18255220]
27. Willmann JK, Lutz AM, Paulmurugan R et al. (2008) Dual-targeted contrast agent for US assessment of tumor angiogenesis in vivo. Radiology 248:936–944 [PubMed: 18710985]
28. Saini R, Hoyt K (2014) Recent developments in dynamic contrast-enhanced ultrasound imaging of tumor angiogenesis. Imaging Med 6:41–52 [PubMed: 25221623]
29. Liu JB, Merton DA, Berger AC et al. (2014) Contrast-enhanced sonography for detection of secondary lymph nodes in a melanoma tumor animal model. J Ultrasound Med 33:939–947 [PubMed: 24866601]
30. Willmann JK, Paulmurugan R, Chen K et al. (2008) US imaging of tumor angiogenesis with microbubbles targeted to vascular endothelial growth factor receptor type 2 in mice. Radiology 246:508–518 [PubMed: 18180339]
31. Estourgie SH, Nieweg OE, Kroon BB (2004) High incidence of intransit metastases after sentinel node biopsy in patients with melanoma. Br J Surg 91:1370–1371 [PubMed: 15376178]
32. Dekker J, Duncan LM (2013) Lack of standards for the detection of melanoma in sentinel lymph nodes: a survey and recommendations. Arch Pathol Lab Med 137:1603–1609 [PubMed: 24168497]
33. Goydos JS (2013) Who should be offered a sentinel node biopsy for melanoma less than 1mm thickness? J Clin Oncol 31:4385–4386 [PubMed: 24190121]
34. Stoffels I, Morscher S, Helfrich I et al. (2015) Metastatic status of sentinel lymph nodes in melanoma determined noninvasively with multispectral optoacoustic imaging. Sci Transl Med 7:317ra199
35. Deshpande N, Ren Y, Foygel K et al. (2011) Tumor angiogenic marker expression levels during tumor growth: longitudinal assessment with molecularly targeted microbubbles and US imaging. Radiology 258:804–811 [PubMed: 21339349]
36. Leong-Poi H, Christiansen J, Klibanov AL et al. (2003) Noninvasive assessment of angiogenesis by ultrasound and microbubbles targeted to alpha(v)-integrins. Circulation 107:455–460 [PubMed: 12551871]
37. Shelton SE, Lindsey BD, Tsuruta JK et al. (2016) Molecular acoustic angiography: a new technique for high-resolution superharmonic ultrasound molecular imaging. Ultrasound Med Biol 42:769–781 [PubMed: 26678155]
38. Bettinger T, Bussat P, Tardy I et al. (2012) Ultrasound molecular imaging contrast agent binding to both E- and P-selectin in different species. Investig Radiol 47:516–523 [PubMed: 22814589]
39. Davidson BP, Chadderdon SM, Belcik JT et al. (2014) Ischemic memory imaging in nonhuman primates with echocardiographic molecular imaging of selectin expression. J Am Soc Echocardiogr 27:786–793. [PubMed: 24774222]

40. Alonso A, Della Martina A, Stroick M et al. (2007) Molecular imaging of human thrombus with novel abciximab immunobubbles and ultrasound. Stroke 38:1508–1514. [PubMed: 17379828]
41. Shim CY, Liu YN, Atkinson T et al. (2015) Molecular imaging of platelet-endothelial interactions and endothelial von Willebrand factor in early and mid-stage atherosclerosis. Circ Cardiovasc Imaging 8:e002765. [PubMed: 26156014]
42. Dewitte H, Vanderperren K, Haers H et al. (2015) Theranostic mRNA-loaded microbubbles in the lymphatics of dogs: implications for drug delivery. Theranostics 5:97–109. [PubMed: 25553101]
43. Hauff P, Reinhardt M, Briel A et al. (2004) Molecular targeting of lymph nodes with L-selectin ligand-specific US contrast agent: a feasibility study in mice and dogs. Radiology 231:667–673 [PubMed: 15118116]
44. Warram JM, Sorace AG, Saini R et al. (2011) A triple-targeted ultrasound contrast agent provides improved localization to tumor vasculature. J Ultrasound Med 30:921–931 [PubMed: 21705725]
45. Molhoek KR, Erdag G, Rasamny JK et al. (2011) VEGFR-2 expression in human melanoma: revised assessment. Int J Cancer. 129:2807–2815 [PubMed: 21544800]
46. Omoto K, Mizunuma H, Ogura S et al. (2002) New method of sentinel node identification with ultrasonography using albumin as contrast agent: a study in pigs. Ultrasound Med Biol 28:1115–1122 [PubMed: 12401380]
47. Curry JM, Bloedon E, Malloy KM et al. (2007) Ultrasound-guided contrast-enhanced sentinel node biopsy of the head and neck in a porcine model. Otolaryngol Head Neck Surg 137:735–741 [PubMed: 17967637]
48. Xie F, Zhang D, Lin C et al. (2015) Intradermal microbubbles and contrast-enhanced ultrasound (CEUS) is a feasible approach for sentinel lymph node identification in early-stage breast cancer. World J Surg Oncol 13:319 [PubMed: 26585236]
49. Matsuzawa F, Omoto K, Einama T et al. (2015) Accurate evaluation of axillary sentinel lymph node metastasis using contrast-enhanced ultrasonography with Sonazoid in breast cancer: a preliminary clinical trial. Spring 17:509
50. Li L, Mori S, Kodama M et al. (2013) Enhanced sonographic imaging to diagnose lymph node metastasis: importance of blood vessel volume and density. Cancer Res 73:2082–2092 [PubMed: 23333937]
51. Aglita G, Valeri G, Argalia G et al. (2017) Role of contrast-enhanced sonography in the evaluation of axillary lymph nodes in breast carcinoma. J Ultrasound Med 36:505–511 [PubMed: 28098400]
52. Guidi AJ, Berry DA, Broadwater G et al. (2000) Association of angiogenesis in lymph node metastases with outcome of breast cancer. J Natl Cancer Inst 92:486–492 [PubMed: 10716967]
53. Jaeger TM, Weidner N, Chew K et al. (1995) Tumor angiogenesis correlates with lymph node metastases in invasive bladder cancer. J Urol 154:69–71 [PubMed: 7539869]
54. Davis RE, Warnke RA, Dorfman RF (1991) Inflammatory pseudotumor of lymph nodes: additional observations and evidence for an inflammatory etiology. Am J Surg Pathol 15:744–756 [PubMed: 2069212]
55. Brown JR, Skarin AT (2004) Clinical mimics of lymphoma. Oncologist 9:406–416 [PubMed: 15266094]

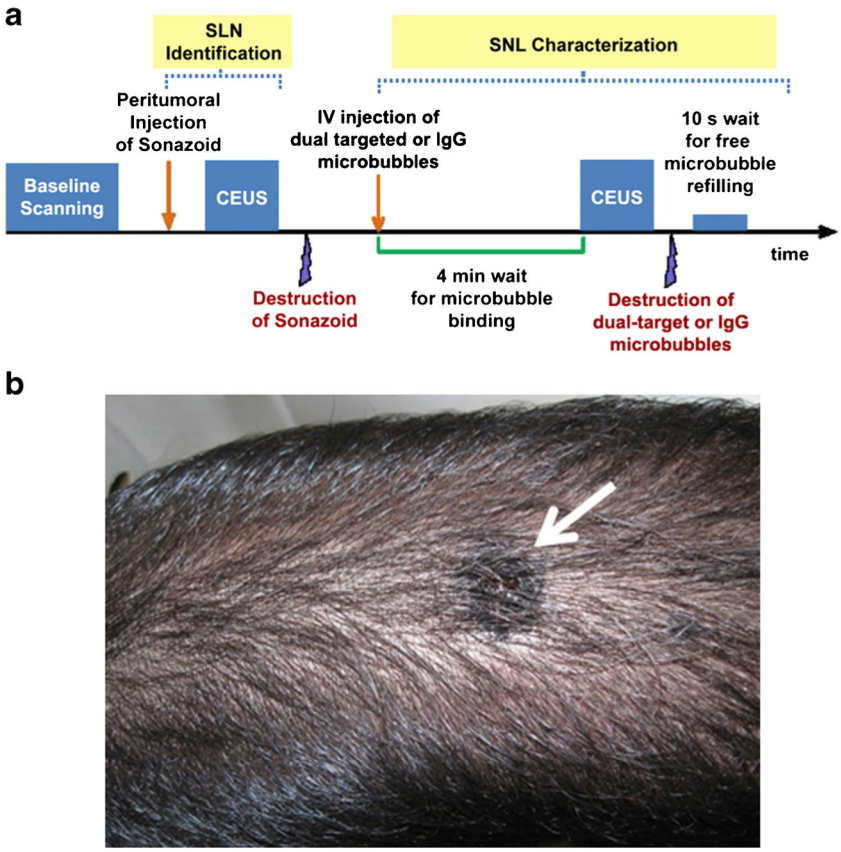

Fig. 1.

a The overview of ultrasound imaging protocol. **b** A melanoma tumor (*arrow*) on a Sinclair swine

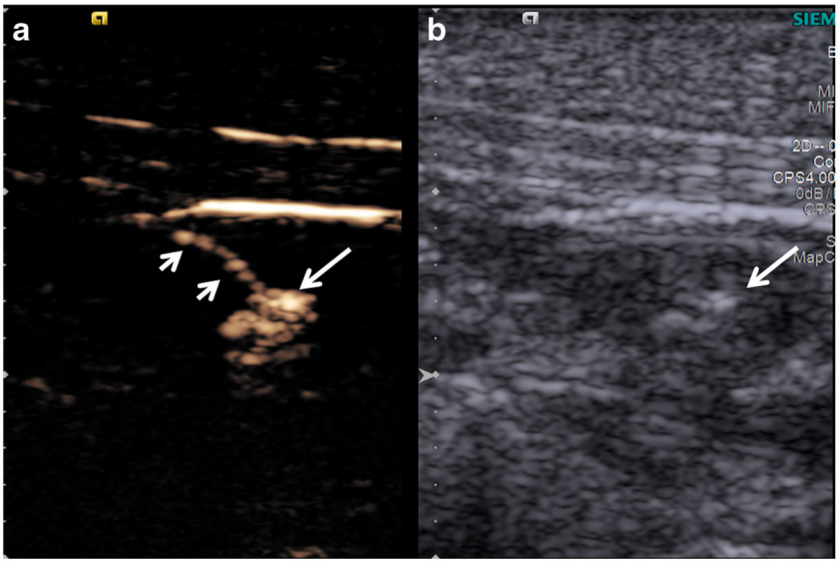

Fig. 2.

a Contrast-enhanced and **b** B-mode images of LC (*short arrows*) and SLN (*long arrow*). The LC and SLN were highly enhanced by Sonazoid and easily visualized.

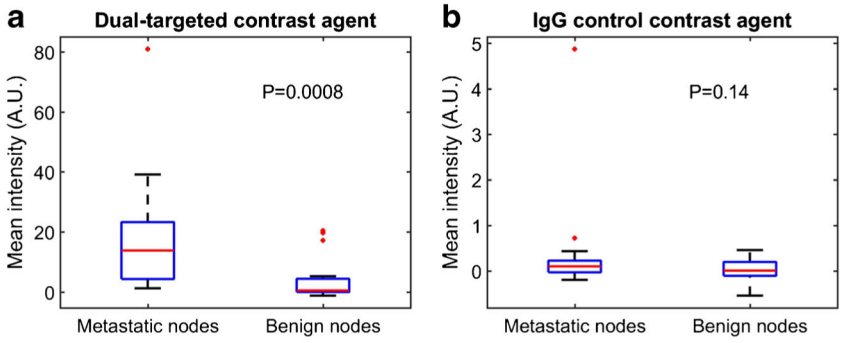

Fig. 3.

Comparison of the mean intensities from **a** dual-targeted and **b** IgG control contrast agents for metastatic and benign nodes (the central mark on each box is the median, the edges of the *box* are the 25th and 75th percentiles, the *whiskers* extended to approximately ±2.7 standard deviation, and outliers are plotted individually).

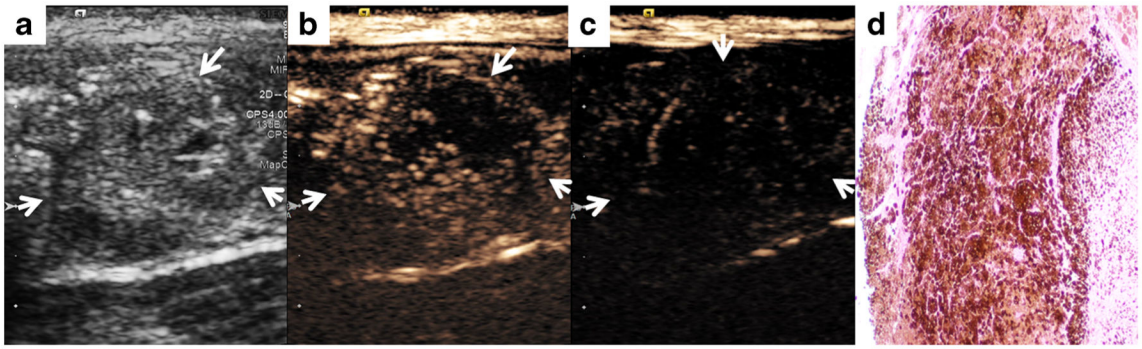

Fig. 4.

A metastatic SLN (*arrows*). **a** B-mode image demonstrates heterogeneous LN with peripheral cystic changes, highly suspicious for metastatic involvement. **b** Contrast-enhanced images with dual-targeted microbubbles and **c** IgG control microbubbles demonstrate extensive preferential retention of dual-targeted microbubbles within the LN. **d** LN histology (HE stain, ×40 magnification) demonstrates extensive metastatic melanoma involvement.

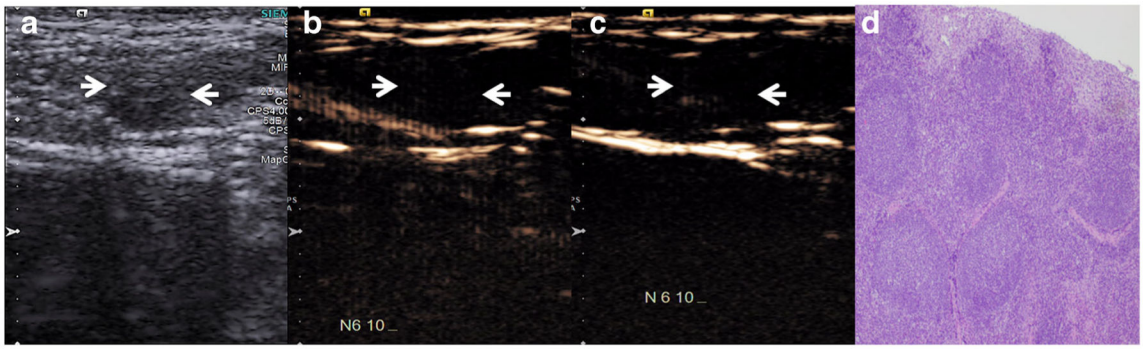

Fig. 5.

A benign SLN (*arrows*). **a** B-mode image demonstrates homogeneous LN with small fatty hilum likely representing reactive LN. **b** Contrast-enhanced images with dual-targeted microbubble and **c** IgG control microbubbles demonstrate no retention of both dual-targeted and control microbubbles within the LN. **d** LN histology (HE stain, ×40 magnification) demonstrates no evidence of metastatic melanoma involvement.

Table 1.

Type and use of ultrasound contrast agents

	SLN identification	SLN characterization	
	Sonazoid	**Dual-targeted**	**Control**
Manufacturer	GE Healthcare, Oslo, Norway	Targeson, San Diego, CA, USA	Targeson, San Diego, CA, USA
Diameter	1–6 μm	2–8 μm	2–8 μm
Composition	Lipid stabilized suspension of perfluorobutane	Streptavidin coated bubble filled with perfluorocarbon (labeled with P-selectin and $\alpha_v\beta_3$-integrin antibodies)	Streptavidin coated bubble filled with perfluorocarbon (labeled with immunoglobulin G)
Administration	Peritumoral injection	IV	IV
Dose	0.25 ml × 4	1.25 ml	1.25 ml